Optoelectronic and nanoelectronic devices

Conference paper
UDC 621.373.826
DOI: https://doi.org/10.18721/JPM.191.114

Beam divergence of surface-emitting semiconductor laser with resonator based on two-dimensional photonic crystal

A.S. Nekrasov [1,2]✉, V.V. Zolotarev [1], I.V. Oreshko [1], S.O. Slipchenko [1], N.A. Pikhtin [1]

[1] Ioffe Institute, St. Petersburg, Russia;

[2] Peter the Great St. Petersburg Polytechnic University, St. Petersburg, Russia

✉ nekrasov.74as@gmail.com

Abstract. Theoretical calculations of the resonator modes optical characteristics of a semiconductor surface-emitting laser with a resonator based on a two-dimensional photonic crystal with a square lattice were carried out in the paper. Photonic crystal provides distributed feedback in plane of heterostructure layers and determines diffraction of radiation to the surface of the laser structure. Output beam emitted in the direction normal to the surface of such devices allows decreasing the beam divergence and increasing the output optical power. However, an increase in radiation aperture also affects the mode composition of the laser emission. The dependences of resonator modes optical losses and beam divergence on cavity size were obtained. A suggestion of the optimal cavity length to achieve single-mode operation with small output laser beam divergence angle was made.

Keywords: photonic crystal, surface-emitting laser, semiconductor laser, resonator, beam divergence

Citation: Nekrasov A.S., Zolotarev V.V., Oreshko I.V., Slipchenko S.O., Pikhtin N.A., Beam divergence of surface-emitting semiconductor laser with resonator based on two-dimensional photonic crystal, St. Petersburg State Polytechnical University Journal. Physics and Mathematics. 19 (1.1) (2026) 86–91. DOI: https://doi.org/10.18721/JPM.191.114

Конференционная статья
УДК 621.373.826
DOI: https://doi.org/10.18721/JPM.191.114

Расходимость лазерного пучка вертикально-излучающего полупроводникового лазера с резонатором на основе двумерного фотонного кристалла

А.С. Некрасов [1,2]✉, В.В. Золотарев [1], И.В. Орешко [1], С.О. Слипченко [1], Н.А. Пихтин [1]

[1] Физико-технический институт им. А.Ф. Иоффе РАН, Санкт-Петербург, Россия;

[2] Санкт-Петербургский политехнический университет Петра Великого, Санкт-Петербург, Россия

✉ nekrasov.74as@gmail.com

Аннотация. В данной работе проведены теоретические расчеты оптических характеристик полупроводникового поверхностно-излучающего лазера с резонатором на основе двумерного фотонного кристалла квадратной симметрии. Фотонный кристалл обеспечивает распределенную положительную обратную связь и дифракцию излучения в направлении нормали поверхности лазерного чипа. Вывод излучения через поверхность позволяет уменьшить расходимость пучка выходного излучения, увеличение апертуры приводит к увеличению выходной оптической мощности.

Однако, увеличение размеров резонатора также влияет на модовый состав излучения. Были получены зависимости оптических потерь резонаторных мод и расходимости пучка от апертуры излучения. Были подобраны оптимальные размеры резонатора для обеспечения одномодового режима работы при малой расходимости пучка выходного излучения.

Ключевые слова: фотонный кристалл, поверхностно-излучающий лазер, полупроводниковый лазер, резонатор, расходимость пучка

Ссылка при цитировании: Некрасов А.С., Золотарев В.В., Орешко И.В., Слипченко С.О., Пихтин Н.А. Расходимость лазерного пучка вертикально-излучающего полупроводникового лазера с резонатором на основе двумерного фотонного кристалла // Научно-технические ведомости СПбГПУ. Физико-математические науки. 2026. Т. 19. № 1.1. С. 86–91. DOI: https://doi.org/10.18721/JPM.191.114

Introduction

Ridge semiconductor lasers have a highly asymmetric wide radiation pattern and multi-mode operation [1], which complicates their application in optoelectronics since expensive collimating optics are required. This problem can be solved by outputting radiation through the surface of a laser device, which is implemented in vertical cavity surface-emitting lasers (VCSELs) [2]. However, VCSELs have a small aperture size due to the design features of the resonator, which limits the high optical output power. Because of this, photonic crystal (PC) surface-emitting lasers (SEL) are developed [3–6], which enabled single-mode high-power output laser emission with symmetrical narrow beam.

Distributed feedback and diffraction to the direction normal to the surface of the device are provided by forming two-dimensional (2D) PC in the heterostructure layers [7]. Optical characteristics of such devices depend on sizes of the resonator, therefore it is important to study this effect.

In this paper theoretical calculation of the mode composition of the resonator based on square lattice 2D-PC has been made. PC is formed by air holes in the layer of heterostructure GaAs/AlGaAs/InGaAs, emitting at a wavelength of 1005 nm. The analysis of dependences of resonator modes optical losses and directional pattern on size of the radiation aperture are carried out.

Materials and Methods

In this paper we studied the heterostructure GaAs/AlGaAs with 3 quantum wells InGaAs. Generated in active layer emission is TE polarized, that is typical for InGaAs. Square lattice PC is formed by air holes in the shape of a right isosceles triangle (RIT) in one of the heterostructure layers (Fig. 1, *a*).

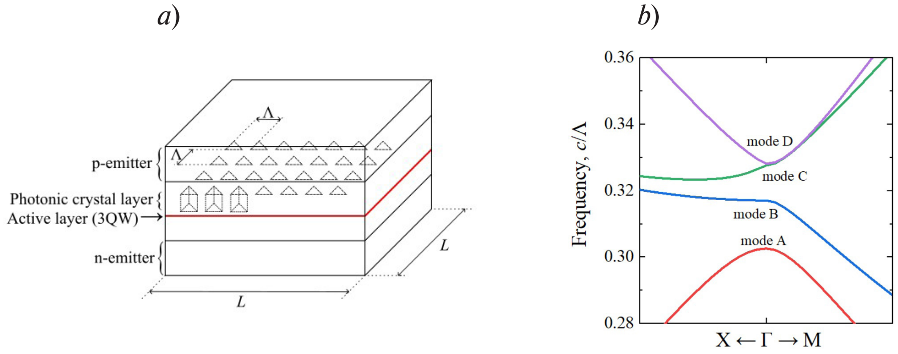

Fig. 1. Schematic structure of SEL device with resonator based on square lattice PC (*a*); typical photonic band structure for square lattice PC with RIT holes (*b*)

PC lattice constant Λ = 300 nm is chosen to satisfy the second-order Bragg's condition, and the holes, whose size is characterized by fill factor $f = S_{air\ hole}/S_{u.c.}$, have f = 22.2%. Calculations of photonic band structure for infinite size square lattice PC shows that in second order Γ-point there are four band-edge modes [8]. We call these modes A, B, C, D (Fig. 1, *b*) in order of increasing frequency.

In order to make the necessary calculations of the resonator's optical characteristics, we utilized coupled-wave model [9]. We will highlight peculiarities of this method: we consider TE polarized wave, for which we have wave equation

$$\nabla \times \nabla \times \vec{E}(\vec{r}) = k_0^2 \tilde{n}^2(\vec{r})\vec{E}(\vec{r}) \quad (1)$$

where $\tilde{n}(\vec{r})$ is the complex refractive index, k_0 is the wavevector of the light in the vacuum. The TE polarization field $\vec{E}(\vec{r}) = (E_x(\vec{r}), E_y(\vec{r}), 0)$ can be expanded in PC due to Bloch theorem:

$$E_i(z) = \sum E_{i,m,n}(z)\exp(-im\beta_0 x - in\beta_0 y),\ i = x, y, \quad (2)$$

where m, n are integers, $\beta_0 = 2\pi/\Lambda$ is the reciprocal lattice vector. The real part of the refractive index can be expanded into a Fourier sum

$$n^2(\vec{r}) = n_0^2(z) + \sum_{m\neq 0, n\neq 0} \xi_{m,n}(z)\exp(-im\beta_0 x + in\beta_0 y), \quad (3)$$

where Fourier coefficients are expressed as

$$\xi_{m,n} = \frac{1}{\Lambda^2}\iint_{PC} \Delta n^2(x,y)\exp(im\beta_0 x + in\beta_0 y)dxdy \quad (4)$$

and equal zero outside of the PC layer. Waves from expansion (2) can be classified based on their wavenumber $\sqrt{m^2+n^2}\beta_0$: basic waves ($m^2 + n^2 = 1$), radiative waves ($m = 0$, $n = 0$) and high-order waves ($m^2 + n^2 > 1$). In the approximation of this model, is suggested that radiative and high-order waves are stimulated by basic waves. The solution of the wave equation (1) for basic waves is reduced to the problem

$$\left(\delta + i\alpha\right)\begin{pmatrix} R_x \\ S_x \\ R_y \\ S_y \end{pmatrix} = C\begin{pmatrix} R_x \\ S_x \\ R_y \\ S_y \end{pmatrix} + i\begin{pmatrix} \partial R_x/\partial x \\ -\partial S_x/\partial x \\ \partial R_y/\partial y \\ -\partial S_y/\partial y \end{pmatrix}, \quad (5)$$

where δ is the deviation of the wavevector from Bragg's wavevector, α is the optical losses, $R_x(x, y)$, $S_x(x, y)$, $R_y(x, y)$, $S_y(x, y)$ – amplitudes of the basic waves propagating in the $+x$, $-x$, $+y$, $-y$ directions accordingly, $C = C_{1D} + C_{rad} + C_{2D}$, C_{1D}, C_{rad}, C_{2D} – matrices, which correspond to one-dimensional coupling, radiative and basic waves coupling, two-dimensional optical coupling accordingly. Problem (5) can be solved using staggered grid finite-difference method with boundary conditions:

$$R_x(0,y) = S_x(L,y) = R_y(x,0) = S_y(x,L) = 0, \quad (6)$$

where L is length of the square resonator (and, accordingly, the radiation apertures). Thereby we obtain set of optical losses of the resonator modes and relative to them values of the basic waves' amplitudes in the grid nodes. We can obtain radiation intensity distribution in near and far fields of the specific mode by utilizing amplitudes of the basic waves [9].

Results and Discussion

In case of RIT holes, modes C and D have much higher threshold losses compared with modes A and B [8], therefore we excluded them from further consideration. We calculated intensity distribution in near and far fields for resonator modes $A_1, L_{1,2}^{A_2}, A_2$ (L = 200 μm, Fig. 2) and $B_1, L_{1,2}^{B_2}, B_2$ (L = 200 μm, Fig. 3) at different cavity lengths. Fundamental modes A_1 and B_1 are characterized by the presence of a single maximum in the center (or close to the center) of the intensity distribution (Fig. 2, *a*, *b*, Fig. 3, *a*, *b*), the smallest beam divergence in their group, and a symmetrical radiation pattern. In contrast, high-order modes have several intensity maximums, which slightly deviate from the normal to the lasing surface (Fig. 2, *c–h*, Fig. 3, *c–h*), that complicates the use of the device. Additionally, high-order modes electromagnetic fields penetrate the boundaries more than fields of fundamental modes, which correspond to higher parasitic losses.

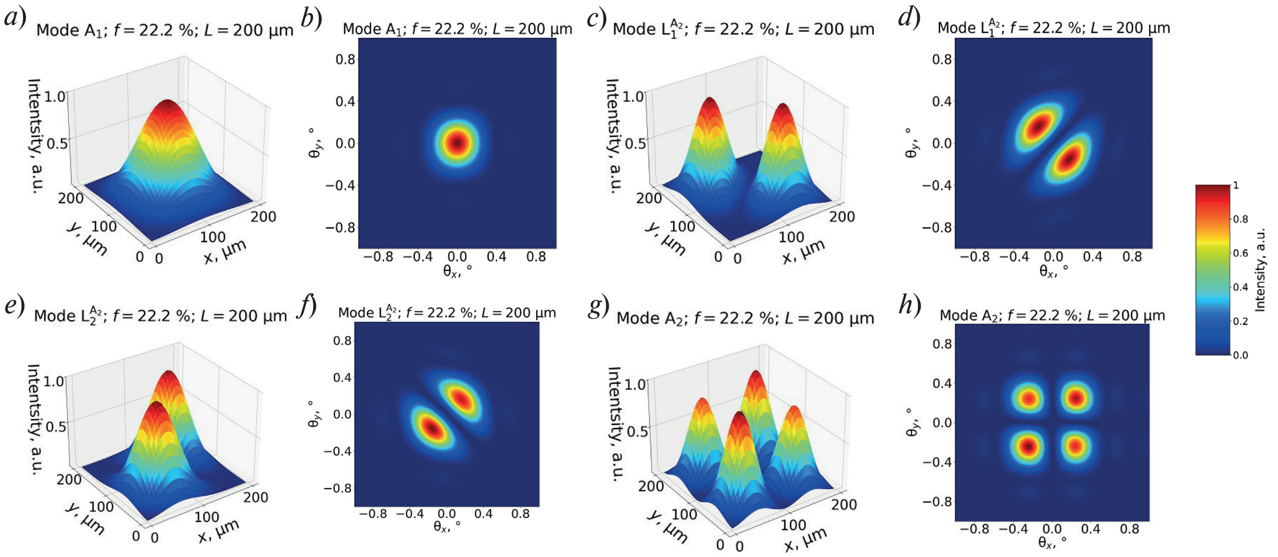

Fig. 2. Radiation intensities of group A resonator modes in near field for fundamental mode A_1 (*a*) and high-order modes $L_1^{A_2}$ (*c*), $L_2^{A_2}$ (*e*), A_2 (*g*) and in far field for A_1 (*b*), $L_1^{A_2}$ (*d*), $L_2^{A_2}$ (*f*), A_2 (*h*). f = 22.2%, L = 200 μm

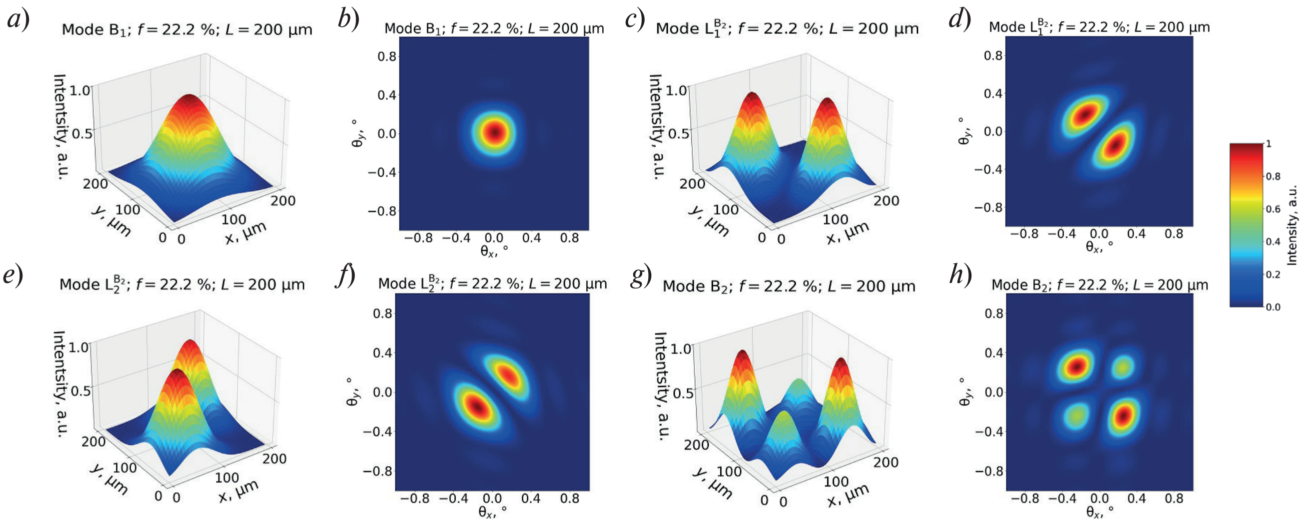

Fig. 3. Radiation intensities of group B resonator modes in near field for fundamental mode B_1 (*a*) and high-order modes $L_1^{B_2}$ (*c*), $L_2^{B_2}$ (*e*), B_2 (*g*) and in far field for B_1 (*b*), $L_1^{B_2}$ (*d*), $L_2^{B_2}$ (*f*), B_2 (*h*). f = 22.2%, L = 200 μm

Using the A_1 mode, we will show the typical changes in the distribution of the radiation intensity of the modes with the change in the size of aperture. PC with holes in the shape of a RIT is characterized by an asymmetry in the intensity envelopes relative to the plane $y = L - x$, which is parallel to the triangle hypotenuse and perpendicular to the plane of the layer. This is especially noticeable at small cavity sizes: at L = 50 μm (Fig. 4, *a*) electromagnetic wave penetrates strongly into the boundaries $x = 0$ and $y = 0$ in comparison to $x = L$ and $y = L$. This leads to reduction in the symmetry of the intensity distribution in far field (Fig. 4, *d*). Increase of resonator length leads to enhancing symmetry of intensity distribution in near and far field (Fig. 4, *b*, *c*, *e*, *f*), because of propagating in plane of PC layer wave manages to fully interact with PC holes, that also provides improvement of resonator properties. Besides this, increase of the radiation aperture leads to narrowing of the output beam in far field: at L = 50 μm, full width at half maximum FWHM = 1.33°, at L = 200 μm, FWHM = 0.35°, at L = 400 μm, FWHM = 0.17°. A similar situation is observed for mode B_1.

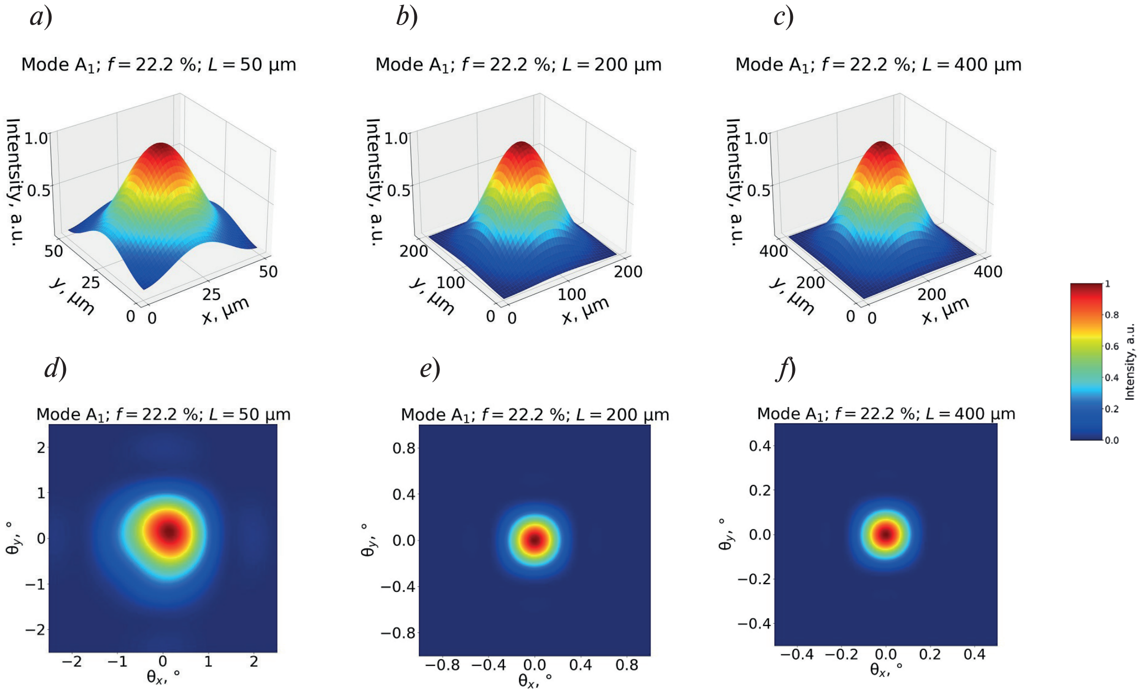

Fig. 4. Radiation intensity distributions of mode A_1 in near field at L = 50 μm (*a*), L = 200 μm (*b*), L = 400 μm (*c*) and in far field at L = 50 μm (*d*), L = 200 μm (*e*), L = 400 μm (*f*)

However, increase of the cavity length leads to weakening of mode discrimination, which is shown in the dependence of resonator modes optical losses on cavity length at Fig. 5, *a*. Thus, mode selection has a value of 100 cm^{-1} at L = 50 μm, and 4 cm^{-1} at L = 400 μm. Meeting the threshold generation condition for several modes will lead to a loss of single-mode operation, and the generation of high-order modes will lead to a significant increase in the divergence of the output beam (Fig. 5, *b*), as well as to loss of the beam pattern symmetry. It is also important to note that a change of the lowest threshold mode ($A_1 \rightarrow B_1$) occurs at L = 140 μm.

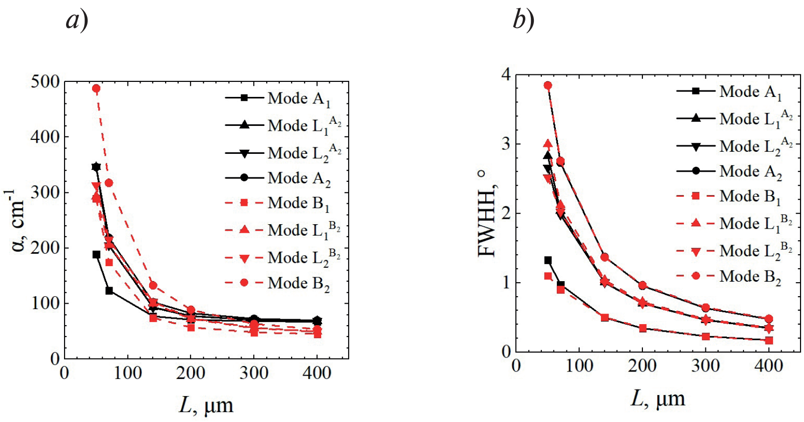

Fig. 5. Resonator modes optical losses dependence on cavity length (*a*).
Beam divergence angle dependence on radiation aperture (*b*)

Conclusion

We have made theoretical calculations of dependences of radiation pattern on cavity length for SEL with resonator based on square lattice PC. The results show that growth of the radiation aperture leads to decrease of beam divergence angle, along with improvement of pattern symmetry. However, this also provides weakening of mode composition selection, as a result, single-mode operation is lost. Based on the results we can suggest optimal cavity length for studied heterostructure, which saves single-mode operation, but provides small beam divergence, specifically at L = 200 μm mode discrimination has large enough value of 14 cm^{-1}, and threshold mode B_1 radiation has beam divergence angle of 0.35°.

REFERENCES

1. **Shashkin I.S. et al.,** Light characteristics of narrow-stripe high-power semiconductor lasers (1060 nm) based on asymmetric AlGaAs/GaAs heterostructures with a broad waveguide, Semiconductors. 54 (4) (2020) 408–413.
2. **Peng C.Y., Tsao K., Cheng H.T., Feng M., Wu C.H.,** Investigation of the current influence on near-field and far-field beam patterns for an oxide-confined vertical-cavity surface-emitting laser, Optics Express. 28 (2020) 30748–30759
3. **Imada M., Noda S., Chutinan A., Tokuda T., Murata M., Sasaki G.,** Coherent two-dimensional lasing action in surface-emitting laser with triangular-lattice photonic crystal structure, Appl. Phys. Lett. 75 (1999) 316–318.
4. **Noda S., Yokoyama M., Imada M., Chutinan A., Mochizuki M.,** Polarization mode control of two-dimensional photonic crystal laser by unit cell structure design, Science. 293 (2001) 1123–1125.
5. **Vurgaftman I., Meyer J.R.,** Design optimization for high-brightness surface-emitting photonic-crystal distributed-feedback lasers, IEEE J. Quantum Electron. 39 (2003) 689–700.
6. **Hirose K., Liang Y., Kurosaka Y., Watanabe A., Sugiyama T., Susumu Noda S.,** Watt-class high-power, high-beam-quality photonic-crystal lasers, Nature Photonics. 8 (2014) 406–411.
7. **Liang Y., Peng C. Sakai K., Iwahashi S., Noda S.,** Three-dimensional coupled-wave model for square-lattice photonic crystal lasers with transverse electric polarization: A general approach, Physical Review. 84 (2011) 195119.
8. **Oreshko I.V., Zolotarev V.V., Slipchenko S.O., Kazakova A.E., Pikhtin N.A.,** Resonators of IR lasers based on two-dimensional photonic crystals for organization of surface output of radiation, Semiconductors. 59 (2) (2025) 109–116.
9. **Liang Y., Peng C., Sakai K., Iwahashi S., Noda S.,** Three-dimensional coupled-wave analysis for square-lattice photonic crystal surface emitting lasers with transverse-electric polarization: finite-size effects, Optics Express. 20 (14) (2012) 15945–15961.

THE AUTHORS

NEKRASOV Aleksey S.
nekrasov.74as@gmail.com

ZOLOTAREV Vasily V.
zolotarev.bazil@mail.ioffe.ru

ORESHKO Ivan V.
ioreshko@mail.ioffe.ru

SLIPCHENKO Sergey O.
serghpl@mail.ioffe.ru
ORCID: 0000-0003-4851-3641

PIKHTIN Nikita A.
nike@hpld.ioffe.ru

Received 16.12.2025. Approved after reviewing 10.02.2026. Accepted 12.02.2026.